Deterministic shape control in plasma-aided nanotip assembly

Cite as: J. Appl. Phys. **100**, 036104 (2006); https://doi.org/10.1063/1.2219378
Submitted: 14 April 2006 . Accepted: 18 May 2006 . Published Online: 10 August 2006

E. Tam, I. Levchenko, and K. Ostrikov

Deterministic shape control in plasma-aided nanotip assembly

E. Tam, I. Levchenko, and K. Ostrikov[a)]
School of Physics, The University of Sydney, New South Wales 2006, Australia

(Received 14 April 2006; accepted 18 May 2006; published online 10 August 2006)

The possibility of deterministic plasma-assisted reshaping of capped cylindrical seed nanotips by manipulating the plasma parameter-dependent sheath width is shown. Multiscale hybrid gas phase/solid surface numerical experiments reveal that under the wide-sheath conditions the nanotips widen at the base and when the sheath is narrow, they sharpen up. By combining the wide- and narrow-sheath stages in a single process, it turns out possible to synthesize wide-base nanotips with long- and narrow-apex spikes, ideal for electron microemitter applications. This plasma-based approach is generic and can be applied to a larger number of multipurpose nanoassemblies. © *2006 American Institute of Physics*. [DOI: 10.1063/1.2219378]

Nanotiplike nanoassemblies have recently been in the spotlight of nanomaterials and nanoelectronics R&D owing to their unique and tunable structural and electronic properties and outstanding flexibility to functionalization and eventual nanodevice integration.[1,2] Ordered arrays of C, Si, W, WO_3, GaAs, GaP, and Al nanotips with different shapes and capping/functional overcoats have been successfully synthesized and tested in various applications.[3–11] In particular, nanotips can be used in nonvolatile data storage elements, interconnects in nanoelectronic integrated circuits, electron emitting and lasing optoelectronic functionalities, nanoplasmonic and photonic devices, biosensors, bioscaffolds, protein and cell immobilization arrays, and some others.[1,2,12] The major issues that still await their solutions are related to deterministic (highly controllable and predictable) nanotip synthesis and nanodevice integration.

It is crucial to select the most suitable nanofabrication process and optimize the synthesis parameters to achieve the desired size and shape (which in turn determine the electronic and some other properties) and also position individual nanotips in the specified device locations. The success of this endeavor depends on the nanoassembly technique. Neutral gas routes (NGRs), such as various modifications of the chemical vapor deposition (CVD), molecular beam epitaxy, and cluster beam deposition, are among the preferred fabrication methods. However, the degree of shape tunability still remains below the expectations of the as yet elusive deterministic nanofabrication. For example, CVD-synthesized conical or pyramidlike carbon nanotips frequently appear short and wide and also lack vertical alignment. This compromises their applications as electron microemitters, which, in particular, demand vertically aligned, sharp and high-aspect ratio nanostructures.[13]

By using a higher-complexity, plasma-enhanced CVD (PECVD) one can dramatically improve nanotip vertical alignment.[3,5] Here, in a numerical experiment that involves a multiscale hybrid Monte Carlo (gas phase) and self-organization of adatoms on the surface numerical simulations, we show that by manipulating the width of the plasma sheath one can effectively tune the shape, size, and features (such as the apex angle, capping, and base radii) of the nanotips. In particular, by applying a sequence of unipolar bias voltages to the growth substrate, it appears possible to synthesize a conical convex-shaped nanoassembly with a base width of ~150 nm, height of ~1 μm, and an apex angle of only 2°–3°, a perfectly shaped nanotip that fits the requirements for the optimized electron field emission.[13]

Here we consider a biased nanostructured substrate immersed in a low-temperature, weakly ionized plasma, created, for example, in a rf, microwave, or dc discharge (Fig. 1). It is assumed that the substrate surface is covered with the initial (seed) pattern of cylindrical nanotips with base radii of 50 nm and height of 300 nm. The presheath potential drop ($\sim T_e/2$, where T_e is the electron temperature) does not exceed a few eV and is neglected. In the sheath region, positive ions are accelerated toward the surface by the sheath potential drop ($\sim U_s$, where U_s is the dc substrate bias). Close enough to the surface, the ions are driven by the local (microscopic) electric fields created by the nanotip array.

Our multiscale numerical simulations incorporate three physical/numerical models: (i) microscopic ion flux topography in the immediate vicinity of the substrate surface and nanotip lateral surfaces (ion motion model) based on the Monte Carlo (MC) technique, (ii) self-organization of adsorbed atoms (adatoms) on the substrate surface not covered by the nanotips (surface condition-controlled adatom diffusion), and (iii) model of the nanotip growth.

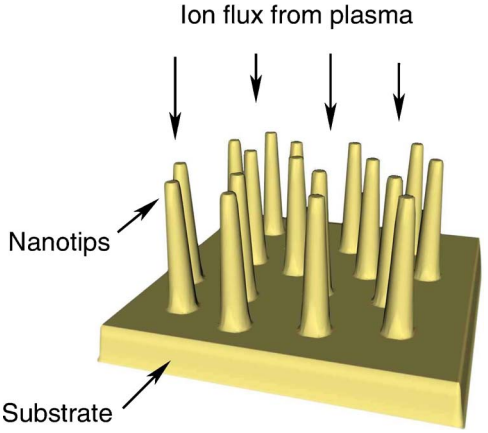

FIG. 1. (Color online) Schematics of nanotip growth.

[a)]E-mail: k.ostrikov@physics.usyd.edu.au

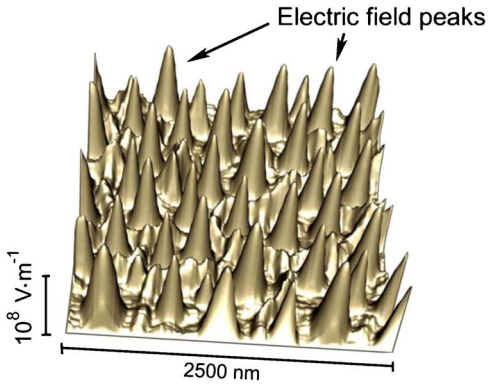

FIG. 2. (Color online) Representative microscopic topography of electric fields in the nanotip pattern.

In the simulation of the microscopic ion flux topography, each nanotip in the pattern was split into 50 horizontal segments to enable the calculation of the ion current density distribution along the lateral surface. Further details of the ion motion model, electric field calculation, and numerical Monte Carlo technique are described elsewhere.[14,15] The growth model is generic and uses the assumption that the energy of ions impinging on the lateral surface of a nanotip is sufficient enough for activation of hydrogen-terminated surface bonds. Moreover, it is assumed that an ion that hits the nanotip surface instantly incorporates into the growing nanostructure at the collision point. By using the discrete vector of the ion current density distribution generated by the MC simulation, one can calculate the dynamic variation of the radius of each nanotip segment $(\partial V_i/\partial r_i)dr_i=J_{di}dt$, where r_i is the radius of the ith segment of the nanotip, J_{di} is the ion flux density on the segment surface (in $\mathrm{m}^{-2}\ \mathrm{s}^{-1}$), and V_i is the volume of the ith segment.

Ionic and neutral species that precipitate on the surface not covered with the nanostructures ("free surface") form a layer of adsorbed species (for simplicity termed adatoms here) that diffuse about the free surface and also participate in the nanotip growth.[16] In the calculation of the diffusion fluxes, we have assumed that the surface diffusion activation energy is $\varepsilon_d \sim 0.6$ eV, which is the case for carbon adatom migration on Si(100) surface heated to a typical substrate temperature $T_s=700$ K. Further assuming that the shape of each nanotip segment is close to cylindrical, the growth equation becomes $r_i(t)=\int_0^t J_i\lambda^3 d\tau$, where λ is the lattice constant and J_i is the total incoming flux of building units to the nanotip surface. This flux consists of the direct ion flux J_{di} and the diffusion influx of adatoms to the circular nanotip borders on the substrate plane. A resultant surface of the nanotip has been computed as an enveloping curve for the discrete radii. It is noteworthy that local electric fields significantly redistribute the ion flux between the nanotip surfaces and open surface areas. In fact, this also affects the nanotip growth by changing diffusion influxes of adatoms to each individual nanotip. Owing to relatively low energy of adsorbed species, it is reasonable to assume the exponential distribution of adatoms over the nanotip height, with the maximum at the substrate surface $(z=0)$. For simplicity, the adatom contribution to the nanotip growth was also incorporated into the total influx J_i.

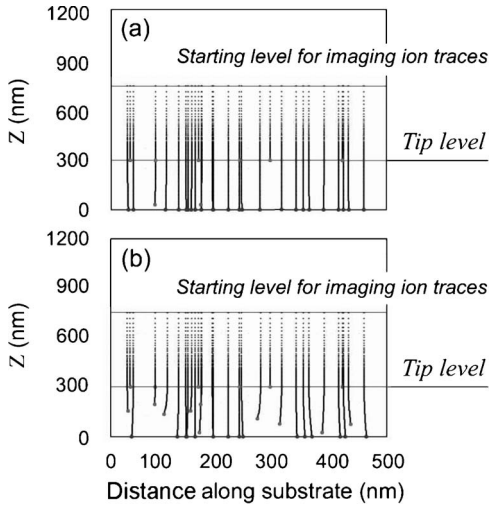

FIG. 3. (a) $T_e=2$ eV, $U_s=50$ V, and plasma density $n_p=4.5\times10^{17}$ m^{-3} (wide sheath). Trajectories mainly linear, ions land on the top of nanostructures or hit the substrate: (b) $T_e=2$ eV, $U_s=20$ V, and $n_p=1.5\times10^{18}$ m^{-3} (narrow sheath). Trajectories curved, a significant amount of ions hits lateral nanotip surfaces.

A representative pattern of the microscopic electric field above the nanotip array is shown in Fig. 2. This figure shows the magnitude of the electric field **E** in the plane $z=2$ μm parallel to the substrate surface. The high peaks of the electric field (reaching 10^8 V/m in the case considered) reveal the positions of the individual nanostructures. A very strong irregularity of the local electrical field leads to a notable ion deflection from straight downfall paths, as shown in Fig. 3. It can be seen that the deflections are small when the plasma sheath is wide [Fig. 3(a)] and become more pronounced when the sheath width decreases [Fig. 3(b)].

The shapes of nanotips for the two different process conditions ($T_e=2$ eV, $U_s=20$ V, and $n_p=1.5\times10^{18}$ m^{-3} and $T_e=2$ eV, $U_s=50$ V, and $n_p=4.5\times10^{17}$ m^{-3}) are shown in Fig. 4. The denser plasma case features a quasiuniform distribution of the ion flux along the nanotip height [Fig. 4(a)]. Complemented by the diffusion influx of adatoms to the nanotip border, this leads to the wide tip formation with a rounded cap and a large apex angle. The second numerical experiment, conducted in the plasma of a lower density, provides an increased influx of the ions to the nanotip base and thus leads to the formation of the capped tip with a very wide base [Fig. 4(b)].

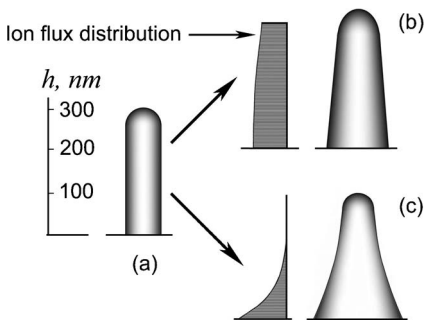

FIG. 4. Two nanotip reshaping processes: (a) original (seed) nanotip, (b) $T_e=2$ eV, $U_s=20$ V, and $n_p=1.5\times10^{18}$ m^{-3}, and (c) $T_e=2$ eV, $U_s=50$ V, and $n_p=4.5\times10^{17}$ m^{-3}.

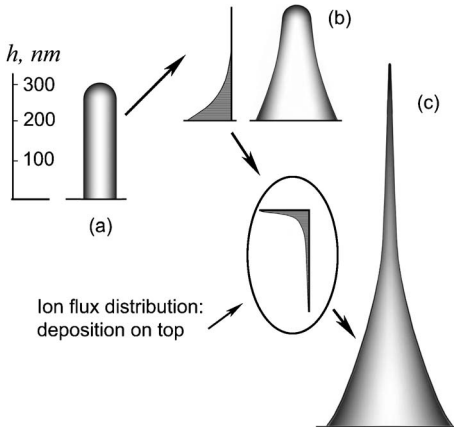

FIG. 5. Reshaping nanotips in a two-stage process: (a) original nanotip, (b) formation of the nanotip base (T_e=2 eV, U_s=50 V, and n_p=4.5×10^{17} m^{-3}), and (c) formation of the emissive spike (T_e=2 eV, U_s=20 V, and n_p=10^{17} m^{-3}).

We now discuss how the sheath width can be controlled and affect the nanotip shape. The width of the plasma sheath depends on the bias voltage, plasma temperature and plasma density and is the main factor in determining the microscopic topology of the ion flux.[17] Ions entering the sheath with a finite velocity (about a few eV, according to the presheath potential drop $\sim T_e/2$) begin to accelerate in the direction normal to the substrate towards the substrate. If the sheath is large compared with the mean nanotip height, the ions acquire the energy corresponding to the sheath potential drop in the upper layer of the sheath where the influence of the electric field produced by the individual nanotips is weak. As a result, the ions will acquire an almost total sheath energy ($\sim U_s$) when entering the irregular electrical field above the nanotip pattern and will not deflect in the local fields of the individual nanotips. On the other hand, under the narrow-sheath conditions, the ions will have a lesser energy when approaching the nanotip surface, and the electric field created by the nanopattern will deflect low-energetic ions. As a result, in the wide-sheath case the ion trajectories are mostly straight lines [Fig. 3(a)], and the ions land on the top of nanostructures or hit the substrate without colliding with the lateral nanotip surfaces. In the narrow-sheath case the ion trajectories are curved [Fig. 3(b)], and a significant amount of ions incorporates into the growing nanostructures via lateral surfaces. This difference in ion energies and trajectories is decisive in the nanotip shape control.

Thus, by appropriately manipulating the plasma parameters, one can effectively control the nanotip shape. However, as can be seen from Fig. 4, none of the growth processes (with either a wide or a narrow sheath) produces the optimum nanotip shape (with a wide base and a sharp tip) for microemitter applications. Indeed, either the base is not wide enough [Fig. 4(b)] or the tip is not sharpened [Fig. 4(c)]. A possible solution to this problem is to combine the above two processes: the first one with a wider sheath to form a wide base first, and then, by narrowing the sheath, shape up a thin and sharp top (Fig. 5). The process depicted in Fig. 5 is an example of sophisticated deterministic nanotip shape control in plasma-aided nanofabrication. Combining two stages that form a wide base firstly, and then a thin low-apex top, one can obtain an optimal nanotip microemitter structure[13] with a low electrical resistance, high mechanical strength, rigidity, and very high electron emission current from the emission spike [Fig. 5(c)]. During the first stage the process is carried on at a substrate bias voltage of 50 V, electron temperature of 2 eV, and the plasma density of 4.5×10^{17} m^{-3}. In this case, the focusing of the ions is weak, and the nanotips mainly grow due to the diffusion fluxes over the substrate surface and by direct ion incorporation into the nanotip base. At the second stage (T_e=2 eV, U_s=20 V, and n_p=10^{17} m^{-3}), narrow-sheath conditions cause a strong focusing of the ions to the upper part of the nanotips close to the top. As a result, a high and narrow spike grows atop of the wide-based nanotip shown in Fig. 5(c).

In summary, the multiscale hybrid numerical simulation was used to study the nanotip shape control in plasma-assisted nanofabrication. Manipulation of the main plasma parameters appears to be an efficient "turning knob" in the deterministic synthesis of the multipurpose nanotip arrays. The strong (up to $\sim$100 V/m) and plasma parameter-dependent dc electric field in the sheath is a crucial factor (absent in NGRs) that enables a certain degree of deterministic synthesis of the desired nanopatterns. By using multistage processes and adopting specific sequences of the plasma parameters, one can create a virtually unlimited continuum of exotic shapes. This approach may be applicable to a much wider range of nanoassembly synthesis and postprocessing and warrants an experimental verification in the near future. This work was supported by the ARC and the University of Sydney.

[1] A. Hellemans, Science **273**, 1173 (1996).
[2] K. Ostrikov, Rev. Mod. Phys. **77**, 489 (2005).
[3] I. B. Denysenko, S. Xu, P. P. Rutkevych, J. D. Long, N. A. Azarenkov, and K. Ostrikov, J. Appl. Phys. **95**, 2713 (2004).
[4] B. T. Liu *et al.*, Appl. Phys. Lett. **80**, 4801 (2002).
[5] C. Bower, W. Zhu, S. Jin, and O. Zhou, Appl. Phys. Lett. **77**, 830 (2000).
[6] Q. Wang *et al.*, Nanotechnology **16**, 2919 (2005).
[7] Z. L. Tsakadze, K. Ostrikov, J. D. Long, and S. Xu, Diamond Relat. Mater. **13**, 1923 (2004).
[8] Z. L. Tsakadze, K. Ostrikov, and S. Xu, Surf. Coat. Technol. **191**, 49 (2005).
[9] C. H. Oon, J. T. L. Thong, Y. Lei, and W. K. Chim, Appl. Phys. Lett. **81**, 3037 (2002).
[10] H. C. Lo, D. Das, J. S. Hwang, K. H. Chen, C. H. Hsu, C. F. Chen, and L. C. Chen, Appl. Phys. Lett. **83**, 1420 (2003).
[11] J. Zhou, L. Gong, S. Z. Deng, J. Chen, J. C. She, N. S. Xu, R. Yang, and Z. L. Wang, Appl. Phys. Lett. **87**, 223108 (2005).
[12] K. Okano, S. Koizumi, S. R. P. Silva, and G. A. J. Amaratunga, Nature (London) **381**, 140 (1996).
[13] L. Nilsson, O. Groening, O. Kuettel, P. Groening, and L. Schlapbach, J. Vac. Sci. Technol. B **20**, 326 (2002).
[14] I. Levchenko, K. Ostrikov, M. Keidar, and S. Xu, J. Appl. Phys. **98**, 064304 (2005).
[15] I. Levchenko, M. Korobov, M. Romanov, and M. Keidar, J. Phys. D **37**, 1690 (2004).
[16] I. Levchenko, K. Ostrikov, M. Keidar, and S. Xu, Appl. Phys. Lett. **89**, 033109 (2006).
[17] I. B. Denysenko, K. Ostrikov, S. Xu, M. Y. Yu, and C. H. Diong, J. Appl. Phys. **94**, 6097 (2003); S. V. Vladimirov and K. Ostrikov, Phys. Rep. **393**, 175 (2004).